Physica Scripta. Vol. T80, 154–157, 1999

Electron-Ion Interactions and Spectroscopy of Highly Charged Ions Studied Using the Tokyo EBIT

F. J. Currell,[1]* D. Kato, N. Nakamura, S. Ohtani,[1] E. J. Sokell,[1] H. Watanabe and C. Yamada[1]

Cold Trapped Ions Project, ICORP, Japan Science and Technology Corporation (JST), Axis Chofu 3F, 1-40-2 Fuda, Chofu, Tokyo 182-0024, Japan
[1] Institute for Laser Science, University of Electro-Communications, Chofu, Tokyo, 182-8585, Japan

Received September 13, 1998; accepted October 20, 1998

PACS Ref: 32.30.Jc 32.30.Rj 34.80.Dp 34.80.Kw 52.25.Jm 52.25.Nr 52.25.Rv 52.25.Wz

Abstract

We have been using the Tokyo EBIT to study a wide range of electron ion interactions and to measure the energies of transitions in highly charged ions. Transition energies were investigated using visible and X-ray spectroscopy. The two electron contribution to the ground state energy of Helium-like Krypton was measured using absorption-edge spectroscopy. Dielectronic recombination processes were measured by mapping the yield of X-rays as a function of electron energy whilst the time dependence of the evolution of charge states was measured, towards the determination of ionization cross-sections. A brief review of these activities is given.

1. Introduction

The first EBIT was constructed by Levine *et al.* [1] to produce highly charged ions and study their X-ray spectroscopy. Two major developments differentiate it from the earlier electron-beam ion source (EBIS) [2]. Firstly, it has a shorter trap to limit instabilities and hence increase the residence time of ions. This increased residence time is the key to producing highly charged ions. Secondly, a pair of superconducting solenoids in the Helmholtz coil configuration is used to compress the electron beam rather than the single solenoid found a typical EBIS. This split coil arrangement facilitates spectroscopy of the trapped ions.

For a number of years, two EBITs have been in operation at Lawrence Livermore National Laboratory. The original EBIT was upgraded (and renamed Super-EBIT [3]) for higher energy operation (0.5 to 210 keV) by floating the gun and collector assemblies. More recently, similar devices have been constructed elsewhere [4–7]. Of all these devices, the Tokyo EBIT [7] is the only 'Super-EBIT' type of device (i.e. the electron gun and collector can float at a considerable potential with respect to laboratory earth). The highest energy this device can be operated at (80 keV) is at present limited by electrical breakdown outside the vacuum system. We are currently constructing a SF6 handling system which should allow us to operate the device at electron energies as high as 340 keV although a period of conditioning is expected before this energy is achieved.

In recent months, our experimental activity has been in three major areas, electron ion interactions (dielectronic recombination and ionization cross section measurements), X-ray (crystal and absorption edge) spectroscopy and visible spectroscopy of highly charged ions. Progress in each of these areas is discussed.

* email fred@ils.uec.ac.jp

2. X-ray Spectroscopy

EBITs are well suited for spectroscopy of highly-charged ions. The ions are at rest to a good approximation, having no centre-of-mass velocity so a Doppler correction is not required. The X-ray source size is defined by the electron beam radius (about 35 μm) and the opening in the drift tubes (about 1 cm long) so this source can be used directly for dispersive spectroscopy without the need for an entrance slit.

We have measured X-ray spectra of Ba, Cs and Xe neon-like ions [8]. These systems are interesting because there is strong mixing of the wave functions in this z-region [9]. Figure 1 shows X-ray spectra measured using a spherically bent quartz crystal [10] and an X-ray sensitive CCD [11] so that both the wavelength and axial source position of emitted photons were recorded. For the data shown in figure 1a, the trap was configured to have the usual square axial potential whereas for that of figure 1b, the potential had a "u-shaped" form. We see that the axial distribution of ions depends on the shape of the axial trapping potential as expected since the ions have an energy distribution.

Assuming the ions of a given charge state have a Maxwellian energy distribution in a state of equipartition, the observed axial ion distribution can be accounted for as follows. The measured distribution can be derived by considering the axial distribution observable by the spectrometer (about +/− 5 mm as determined by the slot in the drift tubes). This 'windowed' distribution is then convolved with the response function of the X-ray spectrometer. The ion temperature can then be varied to give the best agreement with the observed data. This process then gives us a temperature of 9000 + /− 500 eV for Ba^{46+} ions. A comparison of the measured and axial distributions is shown in figure 2. The linear behavior observed near the centre of the trap confirms that the energy distribution of a particular charge state is accounted for by a single Maxwellian distribution and hence a single temperature.

3. Visible Spectroscopy

At lower interaction energies, we have measured visible spectra due to fine-structure transitions of the ground state of Titanium-like ions. Most notably, the $J = 3$ to $J = 2$ transition exhibits anomalous wavelength independence, lying in the visible or near UV region for all atomic numbers greater than 45 [12]. This unusual property makes this transition an ideal diagnostic for fusion devices.

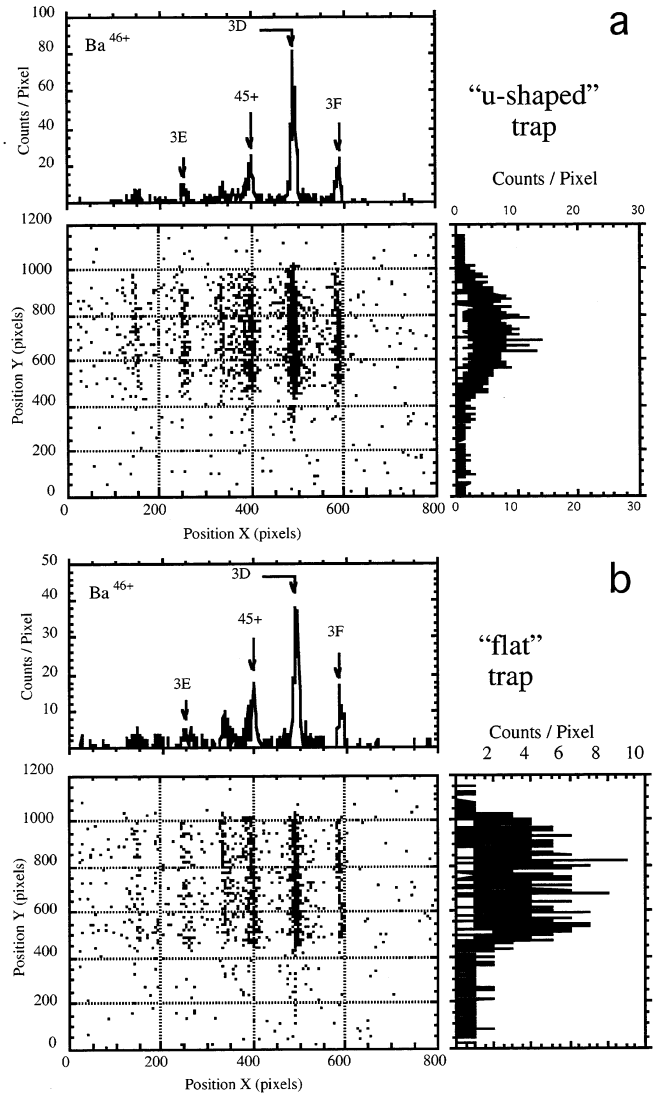

Fig. 1. Spatially and energetically resolved X-ray spectra of trapped Ba^{46+} ions. Fig. 1a shows the spectrum recorded when the trap was configured to have a "u-shaped" potential whilst Fig. 1b shows the spectrum when a more conventional "square" potential was used. In each case, three panels are shown, the largest of which shows the two dimensional image. The two smaller panels show the total signal summed in the appropriate direction to give the spatial distribution (side panels) and a conventional X-ray spectrum (top panels).

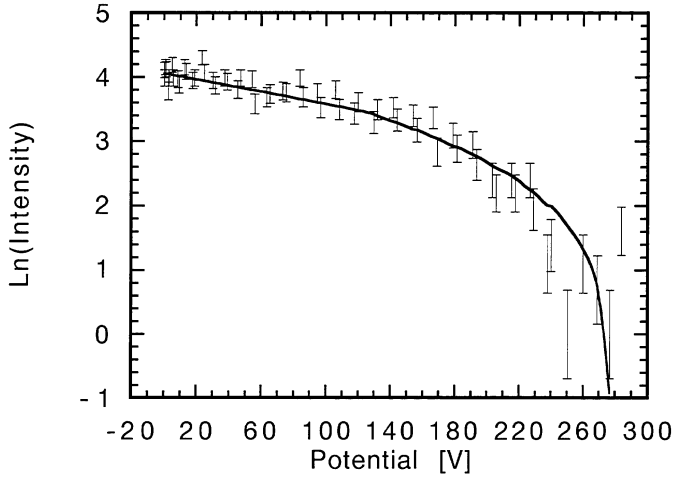

Fig. 2. Natural logarithm of the X-ray intensity (from Fig. 1a) as a function of the potential. The line is the best fit to a model which treats the ion temperature and axial resolution of the spectrometer as adjustable parameters as described in the main text.

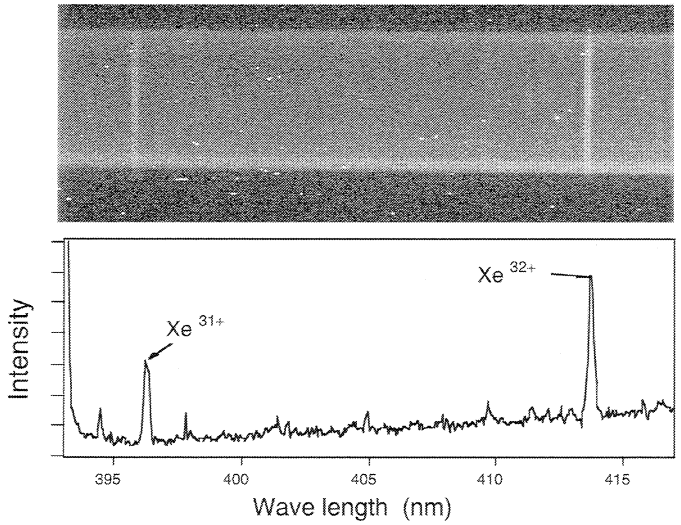

Fig. 3. Visible spectrum of Xenon ions. The upper panel shows the two dimensional image as detected by the CCD. The lower panel shows the wavelengths of observed transitions.

Figure 3 shows an image taken using a Jobin-Yvon visible spectrometer when Xe gas was being injected into the EBIT with an electron beam energy and current of 2.35 keV and 50 mA. Transitions due to Vanadium-like and Titanium-like ions can be observed. These transitions can be distinguished from transitions due to neutrals, which we have observed under different conditions. The ions fill the whole trap giving rise to long features in the vertical (i.e. axial) direction. In contrast, the neutrals are only found at the centre of the trap and hence give rise to shorter features. A detailed comparison between our measurements, previous measurements [13] and theoretical calculations has been performed by Kato *et al.* [14].

4. Variable Interaction Energy Experiments

One of the features of an EBIT is the possibility of varying the electron beam energy to vary the nature of the electron-ion interaction. Figure 4 shows a two dimensional map of detected X-ray intensity as a function of electron energy and X-ray energy. As discussed by Knapp *et al* [15] measurements of this kind show features due to decay of electron impact excited states as vertical lines, radiative recombination (RR) as diagonal lines and dielectronic recombination as the strong features seen at their intersections. This spectrum was taken by periodically rapidly sweeping the electron beam energy after an equilibrium balance of highly charged ions had been created. The electron energies at which X-rays are then detected is recorded with a multiparameter system [11] to produce the map shown in figure 4.

We have exploited the shift of radiative recombination features as the electron beam energy is varied to measure the difference between the binding energies of Helium-like and Hydrogen-like Krypton ions. This difference gives the two-electron contribution to the ground state of Helium-like Krypton (we denote as Δ), which if measured with sufficient accuracy could provide a second order test of two-electron QED effects [16,17]. We measured a two-dimensional map similar to that of figure 4 but in a region free from resonances, with a Lead sheet placed between the solid-state X-ray detec-

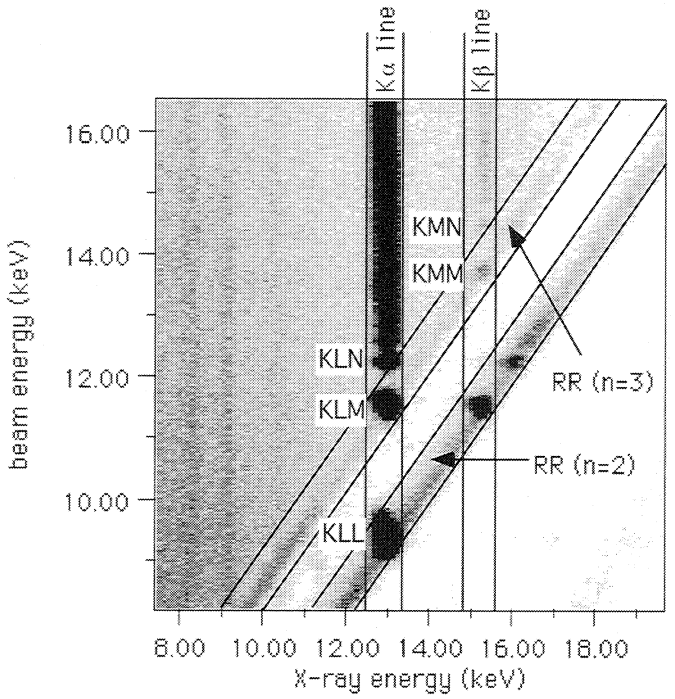

Fig. 4. A spectrum showing the yield of X-rays as a function of electron beam energy and X-ray energy for Helium-like Krypton ions.

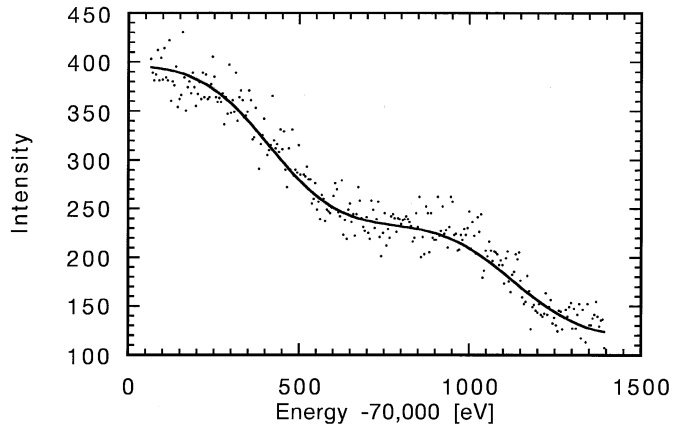

Fig. 5. Intensity of photons due to radiative recombination into Hydrogen-like and bare Krypton ions which subsequently passed through a Lead absorber, as a function of electron beam energy. The points are the measured data and the solid line is the best fit to two error functions. The approximate value of the two electron contribution is indicated as Δ.

tor and the electron beam. The range of interaction energies was chosen so that the features due to $n = 1$ RR into bare and hydrogen-like Krypton both moved through an absorption edge of the Lead sheet. The yield of $n = 1$ RR X-rays is plotted as a function of beam energy in figure 5. The two electron contribution is represented by Δ on this figure. From this preliminary data we have determined a value of $\Delta = 707 + / - 15$ eV. The error bar at present is dominated by the statistical quality of the data. A super-EBIT is ideally suited to this type of measurement since most of the systematic errors cancel, with the final systematic error being determined by the non-linearity of a single power supply (typically 2000 V range) used to sweep the beam energy [18]. Once we take delivery of a larger solid state detector, we hope to make improved measurements of this type, with sufficient precision to test two-electron QED effects to second order.

5. Extracted Ion Based Physics

The Tokyo EBIT is equipped with an ion extraction/transport system [19] which we have used to measure the dynamics of ion creation, including escape rates towards the determination of ionization cross sections. This also constitutes a detailed machine physics study.

The ions in an EBIT are created by successive electron impact ionization steps, starting from neutral gas or low charge-state ions with single ionization being the dominant process. Hence, the time required to create ions of a given charge state is related to ionization cross sections of all the lower charge states. This approach has already been used by Donets and Ovsyannikov [20] to deduce ionization cross sections. The agreement between these measurements and more recent crossed beam measurements [21] is encouraging and suggests that it may be worthwhile trying to extend the technique to more highly charged ions.

For more highly charged ions, there are additional complications associated with charge exchange, radiative recombination, Coulomb collisions and escape of ions from the trap. Although ions are trapped for all positive charge-states, regardless of mass, the volume occupied by ions of a given charge state depends on their temperature. Furthermore, ions can escape from the trap as their temperature becomes comparable to the trapping potential.

All of the processes outlined above can be accounted for [22,23] to predict the time evolution of ions in an EBIT. Solving this model involves calculating the time evolution of many coupled differential equations. Two equations are used for every charge-state of each species present in the trap, one representing the number density and one the temperature. It is however possible to deduce various analytical results from the model which apply under certain conditions. For example, it can be shown that:

$$N_i(t) = (J/e)\sigma^{\mathrm{EI}}_{i-1\to i} f_{i-1} \int_0^t N_{i-1}(t)\,\mathrm{d}t + \epsilon \qquad (1)$$

where $\sigma^{\mathrm{EI}}_{i-1\to i}$ is the ionization cross section from charge state i, $N_i(t)$ is the number of ions of charge state i at time t after the electron beam first starts creating ions, J/e is the current density of the electron beam and f_{i-1} is a measure of the overlap of the ion cloud (of charge state $i-1$) and the electron beam. The term ϵ contains contributions due to processes involving terms $\int_0^t N_i(t)\,\mathrm{d}t$ and $\int_0^t N_{i+1}(t)\,\mathrm{d}t$. These processes have a slower onset than $N_i(t)$ and hence can be distinguished by the behavior of the onsets at early times.

We have measured the time and position of arrival of ions at a detector throughout a cycle which included several 'cooking' periods of different lengths. The full system used to make these measurements is described elsewhere [24]. Essentially, by logging the position of detected ions as a function of time, we determined the time evolution of ions in the trap, including the contribution due to escape. The trap is configured asymmetrically with the trapping potential being significantly smaller in the direction of the ion extraction line. A low trapping potential was used so that the energy required for radial escape was much higher than that for axial escape.

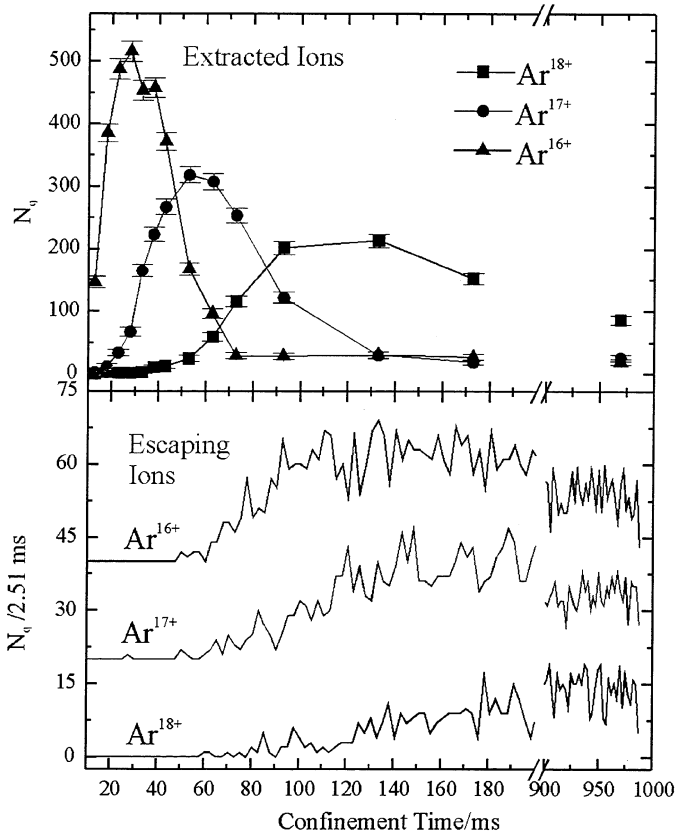

Fig. 6. The measured time dependence of extracted and escaping Argon ions as a function of time. The intensities of extracted ions reflects the charge balance as a function of time whilst the intensities of escaping ions reflects the escape rate as a function of time.

Hence, the measured escape rate should be representative of the actual escape rate at all times. By comparison between the detection rates of escaping and 'dumped' ions it is possible to infer the temperature and hence the size of the ion cloud. Figure 6 shows the time evolution for the creation of Argon ions and the contribution due to escape. In the future, we hope to install a system to measure the electron beam radius, which will allow us to infer absolute cross sections from such data.

Ionization cross section measurements have been made before using an EBIT [25,26] although with a very different method based on the yield of X-rays at equilibrium. It will be interesting to see a comparison of the cross sections measured using the two methods since they pertain to different regimes in the ion time evolution (equilibrium and onset) and hence rely on very different assumptions. Furthermore, the method described here provides estimates of machine physics parameters such as the temperature and cloud size of ions in the trap and the explicit time evolution of ions which may be useful for other experiments (e.g. time resolved spectroscopy of open shell systems).

6. Conclusion

We have performed a number of different studies using the Tokyo EBIT, with interaction energies ranging from 2 keV to 80 keV. Many of these studies are closely related to plasma physics, providing valuable benchmark data as well as being of fundamental interest. Important machine physics has also been investigated as a by-product of these investigations.

Acknowledgements

This work was supported by the Japan Science and Technology Corporation. We gratefully acknowledge helpful discussions with the other members of the YEBISU group and thank Ann Currell for help in preparing this manuscript.

References

1. Levine, M.A., Marrs, R.E., Henderson, J.R., Knapp, D.A., and Schneider, M.B., Physica Scripta **T22**, 157 (1988).
2. Donets, E.D., and Ovsyannikov, V.P., Sov. Phys. JETP **53**, 466 (1981).
3. Knapp, D.A., Marrs, R.E., Elliot, S.R., Magee, E.W., and Zasadzinski, R., Nucl. Instrum. Meth. **334**, 305 (1993).
4. Silver, J.D. *et al.* Rev. Sci. Instrum. **65**, 1072 (1994).
5. Morgan, C. A. *et al.*, Phys. Rev. Lett. **74**, 1716 (1995).
6. Bierdermann, C., Förester, A., Fußmann, G., and Radtke, R., Physica Scripta **T73**, 360 (1997)
7. Currell, F.J. *et al.*, J. Phys. Soc. Jpn **65**, 3186 (1996).
8. Nakamura, N. *et al.*, Physica Scripta *submitted to accompany poster A30 of HCI98* (1998).
9. Kagawa, T., Honda, Y., and Kiyokawa, S., Phys. Rev. A **21**, 7092 (1991).
10. Nakamura, N. *et al.*, Rev. Sci. Instrum. *in press* (1998).
11. Currell, F.J., *et al.*, Physica Scripta **T73**, 371 (1997).
12. Feldman, U., Indelicato, P., and Sugar, J., Opt. Soc. Am. B **8**, 3 (1991).
13. Serpa, F.G. *et al.*, Phys. Rev. A **53**, 2220 (1996).
14. Kato, D. *et al.*, Physica Scripta *submitted to accompany poster A31 of HCI98* (1998).
15. Knapp, D.A. *et al.*, Phys. Rev. Lett. **62**, 2104 (1989).
16. Pesson, H., Salomonson S., Sunnergren, P., and Lindgren, I., Phys. Rev. Lett. **76**, 204 (1996).
17. Marrs, R.E., Elliot, S.R., and Stöhlker, Th., Phys. Rev. A **52**, 3577 (1995).
18. Currell, F.J. *et al.*, J. Phys. B: At. Mol. Opt. Phys., *in preparation* (1998).
19. Motohashi, K. *et al.*, Physica Scripta **T73**, 368 (1997).
20. Donets, E.D., and Ovsyannikov, V.P., Zh. Eksp. Teor. Fiz. **80**, 916 (1981). (Engl. transl. Sov. Phys.-JETP **53**, 466 (1981).)
21. Aichele, K. *et al.*, J. Phys. B: At. Mol. Opt. Phys. **31**, 2369 (1998).
22. Penetrante, B.M., Bardsley, J.N., DeWitt, D., Clark, M., and Schneider, D., Phys. Rev. A. **43**, 4861 (1991).
23. Margolis, H.S., Oxley, P.K., Varney, A.J., Groves, P.D., and Silver, J.D., Physica Scripta **T73**, 375 (1997).
24. Sokell, E.J., Currell, F.J., Shimizu, H., and Ohtani, S., Physica Scripta *submitted to accompany poster B40 of HCI98* (1998).
25. Marrs, R.E., Elliot, S.R., and Schofield, J.H., Phys Rev. A. **56**, 1338 (1997).
26. Stöhlker, Th., Krämer, A., Elliot, S.R., Marrs, R.E., and Schofield, J.H., Phys. Rev. A **56**, 2819 (1997).